pulsed xenon laser," *Appl. Phys. Lett.*, vol. 17, 1970, pp. 305–306.
[8] W. F. Krupke, "Passive *Q*-switching of a CO_2 laser using a mixture of SF_6 and C_2F_3Cl gases," *Appl. Phys. Lett.*, vol. 14, 1969, p. 221.
[9] W. B. Gandrud and R. L. Abrams, "Reduction in SHG efficiency in tellurium by photoinduced carriers," *Appl. Phys. Lett.*, vol. 17, 1970, pp. 302–305.
[10] R. S. Caldwell and H. Y. Fan, "Optical properties of tellurium and selenium," *Phys. Rev.*, vol. 114, 1959, p. 664.

Nonlinear Effects in Inorganic Liquid Lasers

R. R. ALFANO, ALEXANDER LEMPICKI, AND STANLEY L. SHAPIRO

Abstract—**Inorganic liquids, phosphorous, and selenium oxychlorides, used as solvents for Nd, exhibit a number of nonlinear properties, which may reflect in the performance of liquid lasers. Spontaneous and stimulated Raman scattering have been studied. Measured cross sections and gains indicate that up to power levels of a few hundred megawatts per square centimeter the effect on laser and amplifier properties are negligible. No self-focusing has been observed. Under mode-locked conditions substantial conversion to Raman frequencies have been obtained. No connection has been found between stimulated Brillouin scattering and the phenomenon of self-*Q*-switching.**

I. Introduction

RECENTLY inorganic liquid lasers operating at high output energies and powers have been constructed [1]. Solutions of Nd in selenium oxychloride ($SeOCl_2$) or phosphorous oxychloride ($POCl_3$) have been operated in *Q*-switched, self-*Q*-switched, and mode-locked regimes [2]–[7]. Under these conditions the power available inside a liquid laser cavity can be as high as in conventional glass or ruby lasers. Since the active medium is a liquid, however, many of the nonlinear effects associated with the third-order susceptibility can be expected to occur and to affect the laser output.

The nonlinear effects associated with liquids are usually investigated by using high peak power solid-state lasers. Thus the first observation of stimulated Raman scattering was made by placing the nitrobenzene Kerr cell inside the laser cavity to *Q* switch the ruby [8]. Also, saturable absorber liquids are used in *Q*-switched and modelocked lasers [9], and anisotropic molecular liquids can be used to couple modes of solid-state lasers through the optical Kerr effect [10], [11]. Our case differs in that the entire active medium is a liquid and the effects may become "self-generated."

The specific problems that are of interest concern limitations imposed by nonlinearities on the output of liquid lasers. Thus, for instance, generation of stimulated Raman or Brillouin scattering can lead to a power limitation while self-focusing may cause the deterioration of the beam quality and thus limit the usefulness of the liquid laser. Another effect which is particularly easy to observe in liquid lasers is that of self-*Q*-switching. So far no adequate explanation of its mechanism has been given, but the suggestion [4] that it may be due to stimulated Brillouin scattering is not borne out by the present investigation.

In general, the type of effects described here have obvious pertinence to all liquid laser media, including dyes. This paper, however, is limited to the investigation of Raman scattering, Brillouin scattering, and self-focusing in inorganic liquid lasers only.

Manuscript received February 25, 1971.
The authors are with the Bayside Research Center, GTE Laboratories, Bayside, N. Y.

II. Materials

Inorganic laser solutions are multicomponent systems. They consist of a salt of Nd (chloride or fluoroacetate) dissolved in either selenium oxychloride ($SeOCl_2$) or phosphorous oxychloride ($POCl_3$) acidified with a Lewis acid such as tin tetrachloride ($SnCl_4$) or zirconium oxychloride ($ZrCl_4$) [3]. In addition, depending upon the Nd salt and solvent used, some reaction products can be present in solution. In the most commonly used solution, Nd^{+3}:$POCl_3$:$ZrCl_4$, Nd is introduced as a fluoroacetate ($Nd(CF_3COO)_3$). The composition of the solution is (in moles per liter): Nd–0.3; $ZrCl_4$–0.45; $POCl_3$–9; reaction product (dimer) $P_2O_3Cl_4$–0.9. The most abundant component is the oxychloride solvent, and one would expect that the main contribution to nonlinear effects should therefore be determined from the properties of $SeOCl_2$ or $POCl_3$. It should be noted that both of these molecules are highly anisotropic having symmetries of C_s and C_{3v}, respectively, and highly polarizable [12]. One can expect therefore that nonlinearities associated with molecular orientation in strong optical fields may play a role.

III. Spontaneous Raman Scattering

The study of spontaneous Raman scattering has obvious pertinence to our problem since a measurement of

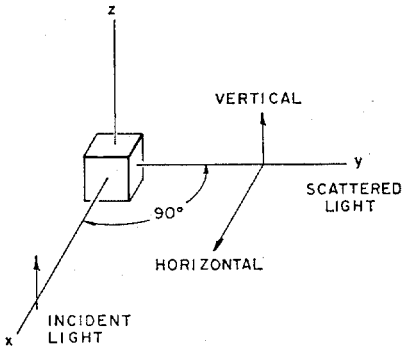

Fig. 1. Geometry of the spontaneous Raman scattering experiment.

the scattering cross section can lead to a theoretical estimate of the stimulated gain. A comparison of calculated and measured gain can in turn shed light on the occurrence of self-focusing. Since data on oxychlorides in the literature [13], [14] are rather qualitative, a quantitative experiment had to be performed.

Spontaneous scattering spectra were obtained by using the geometry shown in Fig. 1. Excitation was provided by the 4880-Å line of argon-ion laser with 50 mW power output and a vertically polarized beam. Radiation scattered at 90° was focused into the slit of a ½-m Jarrell–Ash spectrometer, and detected by an RCA 1P21 photomultiplier, Keithley ammeter, and strip chart recorder. Vertically or horizontally polarized components of the scattered light could be selected by an analyzer. The spectrometer resolution was 0.5 Å or 1.5 cm^{-1}, sufficient to measure the much broader Raman lines of $POCl_3$ and $SeOCl_2$. To provide comparison between the scattering of different liquids, solutions could be placed in identical cells.

Spontaneous Raman spectra of pure $POCl_3$ and pure $SeOCl_2$ are shown in Fig. 2. The most intense lines are the metal–halogen vibrations at 488 cm^{-1} ($POCl_3$) and 386 cm^{-1} ($SeOCl_2$). The 488 cm^{-1} $POCl_3$ line is shown under high resolution in Fig. 3(a). The FWHM was measured to be 5.2 ± 0.8 cm^{-1}. A large fraction of this width is presumably due to the presence of different chlorine isotopes. The line is almost completely polarized vertically with an extinction ratio >30.

Upon addition of the Nd ion and Lewis acid, several changes occur in the spectra of the pure solvents. The 488 cm^{-1} line of $POCl_3$ is reduced in intensity by about 10 percent and a new line appears some 5 cm^{-1} to the red of the 488 cm^{-1} line. This new line, shown in Fig. 3(b), appears to be caused by the addition of the Lewis acid since it is also present in solutions containing no Nd ion. The intensity of the 1297 cm^{-1} line is substantially reduced upon the addition of Nd presumably because it coincides with an absorption due to the ion when the exciting wavelength is 4880 Å.

The most intense feature of the $SeOCl_2$ Raman spectra is the 386 cm^{-1} Se–Cl vibration. Its lineshape in the pure solution and in laser solutions with different Nd^{3+} con-

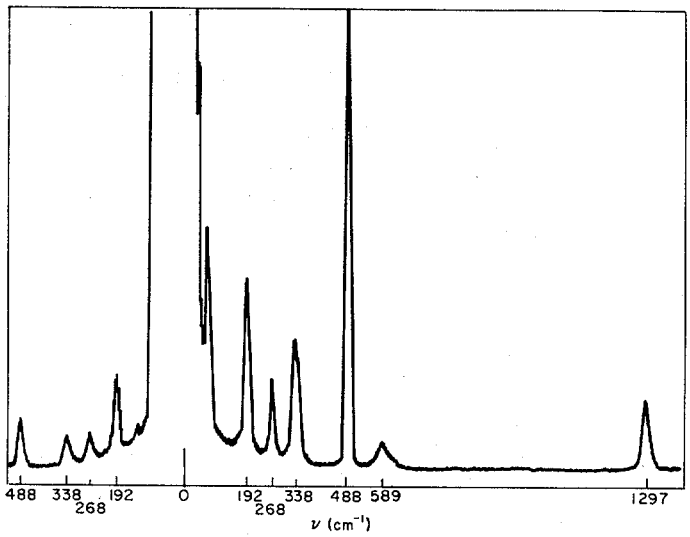

Fig. 2. (a) Raman spectrum of pure $POCl_3$. (b) Raman spectrum of pure $SeOCl_2$.

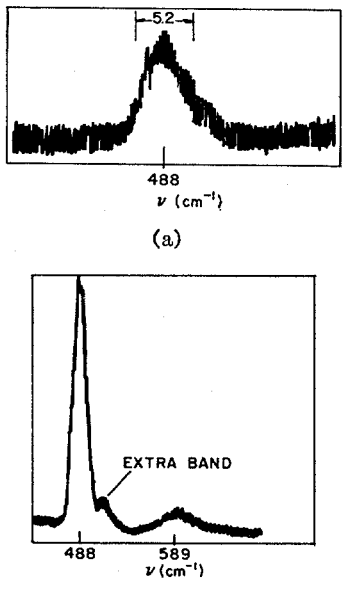

Fig. 3. (a) 488 cm^{-1} vibrational line of $POCl_3$ under high resolution. (b) 488 cm^{-1} line at a faster scan speed showing extra band in laser solution.

centrations is shown under high resolution in Fig. 4. In a pure $SeOCl_2$ solution the 386 cm^{-1} line has a complex structure $\cong$18 cm^{-1} wide and is polarized vertically. In the laser solution of Nd^{3+} $SeOCl_2$, as in $POCl_3$, a new line appears shifted to the red of the 386 cm^{-1} line by $\cong$ 5 cm^{-1}. When Nd^{+++} is removed from the laser solution, the extra line is still present indicating that the ionic complex is not responsible for this new line. At the highest molar concentrations studied (10^{-2} molar), the red shifted line is nearly as intense as the main Raman line.

For the calculation of gain in stimulated Raman scattering, it is necessary to know the magnitude of the *forward* spontaneous scattering cross section per molecule, per unit solid angle $(d\sigma/d\Omega)_{N,\,\theta=180°}$. This quantity is rather difficult to measure absolutely but in some special cases can be deduced from comparative measurements performed at 90°. Such a special case arises if we compare the 488 cm^{-1} and 386 cm^{-1} lines of $POCl_3$ and $SeOCl_2$ with the 656 cm^{-1} Raman line of CS_2. All of these lines are completely polarized and therefore correspond to totally symmetric vibrations [15]. The scattering cross section for vertical polarization is therefore independent of the angle θ [16], [17]. For this special case one can therefore obtain values of the forward scattering cross sections of the oxychlorides, relative to that of CS_2, by using only 90° measurements.

To obtain the cross-section ratios, spectra of the 656 cm^{-1} line of CS_2 were taken in the same apparatus. The measurable quantities such as frequencies, linewidths, and relative peak intensities are then related to the cross section in the following manner. We define [18] a *differential* cross section per unit wavelength interval, per unit solid angle and volume $d^3\,\sigma(\lambda)/d\lambda\,d\Omega dV$. If we assume that the dependence of the cross section is Lorentzian in wave-number space ($\nu = 1/\lambda$) we have:

$$\frac{d\sigma(\nu)}{d\nu} = \left[\frac{d\sigma}{d\nu}\right]_{\nu=\nu_0} \frac{\pi\Delta\nu}{2}\,\frac{\Delta\nu}{2\pi}\,\frac{1}{(\nu-\nu_0)^2+\left(\frac{\Delta\nu}{2}\right)^2}. \tag{1}$$

We can integrate the differential cross section over the linewidth $\Delta\nu$ and volume and obtain

$$\frac{d\sigma}{d\Omega} = \iint \frac{d^3\sigma(\lambda)\,d\lambda\,dV}{d\lambda\,d\Omega\,dV} = \iint \frac{d^3\sigma(\nu)}{d\nu\,d\Omega\,dV}\,d\nu\,dV$$
$$= \left[\frac{d\nu(\nu)}{d\nu}\right]_{\nu=\nu_0} \frac{\pi\Delta\nu}{2}\,V. \tag{2}$$

Using the parameter $K_{\max}$ defined by McClung and Weiner [18], we obtain

$$K_{\max} = \left[\frac{d\sigma(\lambda)}{d\lambda}\right]_{\lambda=\lambda_0} = \nu_0^2\left[\frac{d\sigma(\nu)}{d\nu}\right]_{\nu=\nu_0}. \tag{3}$$

The cross section per molecule is obtained from (2) and (3)

$$\left(\frac{d\sigma}{d\Omega}\right)_N = K_{\max}\,\frac{\pi}{2}\,\frac{\Delta\nu}{\nu_0^2}\,\frac{1}{N}\ (\mathrm{cm}^2/\mathrm{sr}) \tag{4}$$

where N is the number density of the substance.

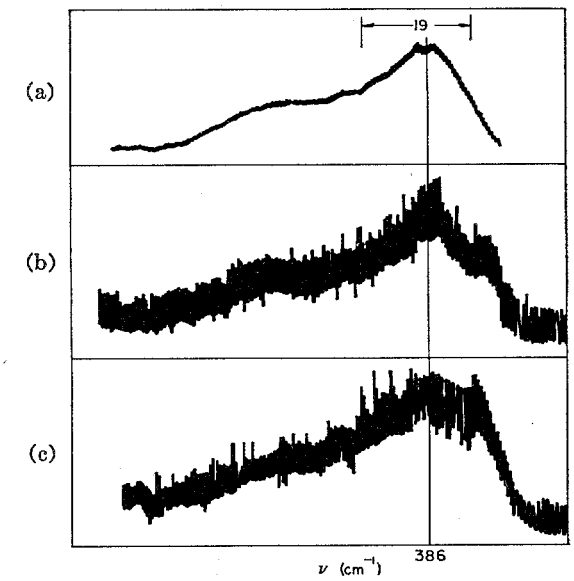

Fig. 4. (a) Raman spectrum of $SeOCl_2$ line at 386 cm^{-1}. (b) 386 cm^{-1} line in 0.3 molar Nd^{+3} laser solution showing side band. (c) 386 cm^{-1} line in 0.6 molar Nd^{+3} laser solution.

Since the quantity $K_{\max}$ is proportional to the peak intensity of the Raman line I_{peak}, we can obtain the ratio of the cross sections of two liquids (*1* and *2*) from a measurement of their peak intensities and linewidth:

$$\frac{\left(\frac{d\sigma}{d\Omega}\right)_{N,1}}{\left(\frac{d\sigma}{d\Omega}\right)_{N,2}} = \frac{I_{\text{peak},1}}{I_{\text{peak},2}}\,\frac{\left(\frac{\Delta\nu}{\nu_0^2}\frac{1}{N}\right)_1}{\left(\frac{\Delta\nu}{\nu_0^2}\frac{1}{N}\right)_2}. \tag{5}$$

The following results were obtained for the relative intensities:

$$\frac{I_{\text{peak}}(POCl_3)}{I_{\text{peak}}(CS_2)} = 0.05 \pm 0.01$$
$$\frac{I_{\text{peak}}(SeOCl_2)}{I_{\text{peak}}(CS_2)} = 0.06. \tag{6}$$

From the linewidth of CS_2 measured by Clements and Stoicheff [19], its cross section taken as 3.8×10^{-29} cm^2 [20], and our measurements of intensity ratios (6) and linewidth, we can obtain the cross sections for the oxychlorides at 4880 Å. These, together with other pertinent data, are given in Table I. To obtain cross sections for other exciting wavelengths, we can use the relationship [21]

$$\left(\frac{d\sigma}{d\Omega}\right)_{\nu_1} = \frac{\nu_1\nu_{S1}^3}{\nu_2\nu_{S2}^3}\left(\frac{d\sigma}{d\Omega}\right)_{\nu_2} \tag{7}$$

where ν_1, ν_2 are the wave number frequencies of the exciting radiation and ν_{S1}, ν_{S2} are the corresponding frequencies of the Stokes lines.

IV. Stimulated Raman and Brillouin Scattering

Stimulated scattering in liquid laser media was obtained in two different ways. For the measurement of

TABLE I
STIMULATED RAMAN SCATTERING DATA FOR OXYCHLORIDES

	$POCl_3$	$SeOCl_2$
Raman shift ν_R	488 cm^{-1}	386 cm^{-1}
Linewidth $\Delta\nu_R$	5.2 cm^{-1}	18 cm^{-1}
Forward scattering cross section ($d\sigma/d\Omega$):		
4880 Å	3.05×10^{-29} cm^2	9.6×10^{-29} cm^2
6940 Å[a]	0.86×10^{-29} cm^2	2.7×10^{-29} cm^2
10 600 Å	0.16×10^{-29} cm^2	0.49×10^{-29} cm^2
Gain coefficient (calculated):[b]		
6940 Å	2.44×10^{-3} cm/MW	2.63×10^{-3} cm/MW
10 600 Å	1.6×10^{-3} cm/MW	1.6×10^{-3} cm/MW
Gain coefficient (measured):		
6940 Å	2.6×10^{-3} cm/MW	-

[a] Calculated from (7).
[b] Calculated from (1) and (7).

spectral shifts and energy conversion, an external laser source (ruby or Nd glass) was used and its output passed through a cell containing the liquid (Sections *A* and *B*). In a second set of experiments the ouput of a liquid laser itself was shown to contain stimulated Raman emission internally generated (Section *C*).

A. Threshold and Energy Conversion

A single transverse and longitudinal ruby laser (Korad) was used for most measurements of energy conversion into stimulated Raman scattering (SRS) and stimulated Brillouin scattering (SBS). The experimental arrangement is shown in Fig. 5. The Korad laser consists of a sapphire etalon output reflector, a 1-mm aperture, a 4-in ruby rod, a Kodak *Q*-switch dye cell antireflection coated at the ruby wavelength, and a 100 percent reflectivity rear-output reflector.

The ruby laser output pulse duration was 15 ns as measured by a TRG detector connected to a Tektronix 519 scope (0.5-μs risetime). Independent measurements of the laser output power with an EGG radiometer and a TRG calorimeter yielded a value of 1 MW. An inverted telescope reduced the beam area size to 0.5 mm^2 across the Raman cell, which was 50 cm long. The output power entering the cell was typically 0.7 MW, thus giving a power per unit area of $\cong$140 MW/cm^2. The Raman cell was several meters from the laser and tilted to minimize optical feedback. Glass microscope slides were placed in the laser beam to vary the power. The beam polarization was perpendicular to the table. The laser output power was monitored before and after the Raman cell as was the forward and backward SRS and SBS. Glass wedges with surfaces parallel to the laser polarization reflected the light upon MgO reflectors. The diffused scattered light from the MgO plates then fell upon RCA 922 phototubes (S1 response) whose outputs were displayed on a 555 Tektronix oscilloscope. Attenuators were placed in front of the tubes so that they operated in a linear response region. The phototube responses were calibrated by conventional techniques. Conversion efficiencies were

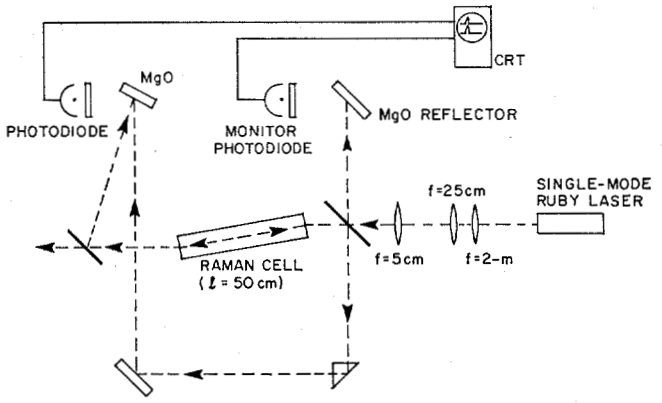

Fig. 5. Experimental arrangement for investigating stimulated Raman and Brillouin scattering.

measured by comparing the pulse heights on the scope. The forward Raman beam was observed by placing Corning 7–69 filters in front of tube 1, and the back Brillouin beam was observed by placing a narrow-band filter in front of tube 2.

Most of the stimulated Raman scattering experiments were carried out with $POCl_3$-based laser solutions. In order to separate the nonlinear effects of the main component ($POCl_3$) from possible contributions of Nd^{+3}, Lewis acid and reaction products, experiments were carried out on pure $POCl_3$, a mixture of $POCl_3$ and $P_2O_3Cl_4$,[1] and in standard laser solution with the Nd^{+3} ion replaced by Eu^{+3}. This replacement was necessary because Nd^{+3} has a strong absorption band at the ruby frequency. The use of a different rare-earth ion was not believed to change any of the relevant properties of the material.

The curve of SRS versus the ruby laser intensity for pure $POCl_3$ is plotted in Fig. 6. Only forward Raman scattering was observed from $POCl_3$. Backward SRS from $POCl_3$ was measured to be $\leq$0.01 of the forward

[1] This mixture was prepared by dissolving $Nd(CF_3COO)_3$ in pure $POCl_3$ and filtering out the Nd containing precipitates. The remainder is believed to contain a mixture of $POCl_3$ and $P_2O_3Cl_4$ in proportion occurring in standard laser solution [22].

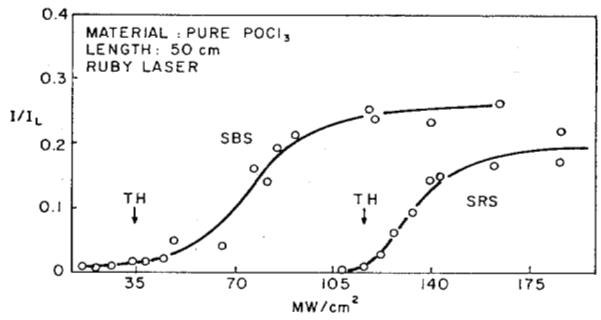

Fig. 6. Stimulated Raman and Brillouin scattering in $POCl_3$ versus ruby laser intensity.

scattering at the power levels of the experiment. Theoretically [23], the forward-to-backward ratio is one, under steady-state conditions, but this value is computed in the absence of backward SBS, which, if present, can compete against the back SRS light.

As seen from Fig. 6, substantial Raman conversion occurs over a length of 50 cm at powers of $\simeq$100 MW/cm^2. From the initial rising portion of the SRS curve, we can calculate the gain of the stimulated process by using the expression

$$I_R \propto I_L \exp(gI_L l) \tag{8}$$

where I_R is the Raman intensity as it leaves the cell and I_L is the intensity of the laser. We obtain $g(POCl_3) = 2.6 \times 10^{-3}$ (cm/MW).

The Brillouin-scattering curve shows that a large amount of laser conversion to SBS takes place at $\simeq$20 MW/cm^2. At powers where substantial Raman conversion begins, approximately 20 percent of the laser has been depleted into backward Brillouin scattering. At the highest laser powers in this experiment, as much as 40 percent of the laser beam is converted to SBS and 30 percent to SRS light.

The curves of the Raman and Brillouin intensities versus laser power reach saturation regions at high powers because of laser depletion into SRS and SBS. The laser depletion was further verified by observing that the laser beam intensity transmitted through the cell decreased as the SBS and SRS built up.

For solutions containing a mixture of $POCl_3$ and $P_2O_3Cl_4$ the only difference in Raman scattering was an increase of threshold by approximately 20 percent. This corresponds roughly to the volume decrease of pure $POCl_3$ caused by the presence of the dimer. When pure $POCl_3$ was doped with its dimer plus europium, the threshold for Raman scattering increased still further. These results show that at laser powers used in these experiments, pure $POCl_3$ is primarily responsible for SRS, and that rare-earth ions and additional liquid components act like inactive participants.

To ascertain if SRS is associated with self-focusing, photographs of SRS light were taken at the end of the cell. No filaments could be detected at the power levels used.

In another series of experiments picosecond pulse excitation was used to produce stimulated scattering. Under these conditions Brillouin scattering usually does not occur and one can expect more efficient conversion into Raman scattering [24]. The experimental set up was similar to that used for observations of self-phase modulation in liquids and solids [25]. It consisted of a mode-locked Nd:glass laser whose output was converted to the second harmonic and the beam collimated to a diameter of 1.2 mm. The energy per pulse was $\sim$5 mJ, pulse duration $\sim$4 ps, and peak power $\simeq$1 GW/cm^2. The output from the cell was passed through a 10-cm focal length lens placed at the focal distance from a 2-cm-high slit of a $\frac{3}{4}$-m Jarrell–Ash spectrograph, and recorded photographically on Polaroid 3000 speed film. Corning filters 5–60 and 5–61 were used to attenuate the fundamental frequency and pass the anti-Stokes shifted light. For observation of Stokes shifted light a 3–67 Corning filter was used. The exposed film containing both spectral and angular [24], [25] information is shown in Fig. 7. As much as eight anti-Stokes and five Stokes stimulated lines could be detected. In all probability the decreasing sensitivity of the Polaroid film limits the number of observable Stokes lines. In addition to the Raman lines a substantial amount of self-phase-modulated emission is seen to form a spectrally continuous and spatially diverging background.

No attempts were made to estimate the energy conversion into Raman and self-phase-modulated radiation under this type of excitation. The results indicate, however, that the use of liquid lasers for amplification of very-high-intensity picosecond pulses may lead to a very complex output.

B. Frequency Shifts Due to SBS

The frequency shift due to SBS was measured in order to elucidate the possible connection of this phenomenon with the self-Q-switching properties of the aprotic laser [4]. The experimental arrangement used for these measurements was similar to that described by Brewer and Shapero [26] and is shown in Fig. 8. A TRG 104 ruby laser Q switched by a rotating prism and cryptocyanine dye was used as a source. A resonant reflector consisting of two sapphire plates produced a single longitudinal-mode output.

The peak power of the pulse was measured by an ITT planar photodiode T_1. Part of the signal reflected from beam splitter B_2 was passed twice through a quarter-wave plate, rotating its polarization by 90°, and was then directed to the Fabry–Perot interferometer. The major part of the signal was focused by a 100-mm focal-length lens L into a 150-mm cell containing the liquid under study.

This lens was used to increase the power density of the ruby radiation, which otherwise was insufficient to produce SBS in Nd-containing solution. As previously noted, an absorption at the ruby frequency made this necessary. The back-scattered radiation from the cell

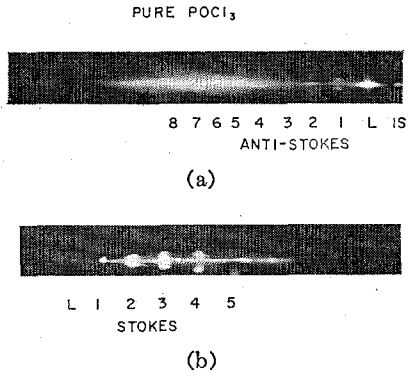

Fig. 7. Angular emission from pure $POCl_3$ under picosecond laser excitation. (a) Anti-Stokes emission. (b) Stokes emission.

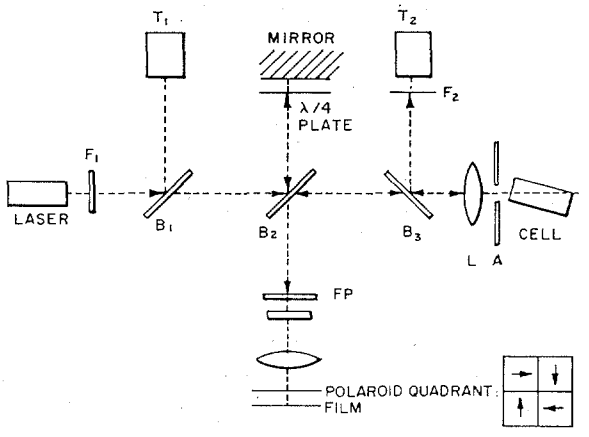

Fig. 8. Experimental arrangement for the measurement of stimulated Brillouin shifts. L—ruby laser; T_1, T_2—planar photodiodes; B_1, B_2, B_3—beam splitters; F_1, F_2—filters; L—lens.

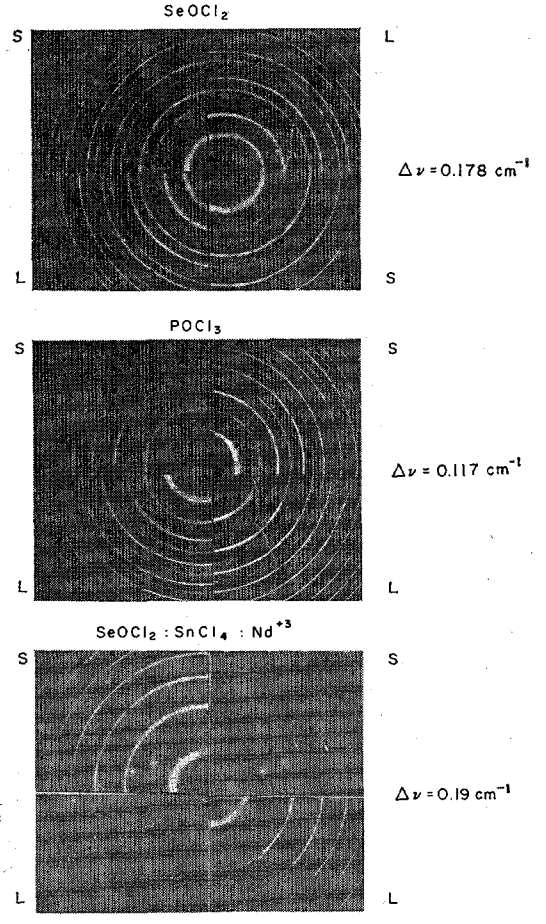

Fig. 9. Interferograms of the incident (L) and scattered (S) radiation. Inter-order spacing for $SeOCl_2$—0.494 cm^{-1}; $POCl_3$—0.27 cm^{-1}; Nd^{+3}:$SeOCl_2$:$SnCl_4$—0.494 cm^{-1}.

was detected by the photodiode T_2, and part of it was allowed to enter the Fabry–Perot interferometer. To distinguish between the incident and scattered radiation, which, upon arrival at the interferometer, are polarized at right angles, a quadrant of sheet polarizers was placed in front of the film.

Typical interferograms of the incident and back-scattered radiation are shown in Fig. 9. Table II gives the measured shifts $\Delta\nu$ for a number of solutions. From $\Delta\nu$ and the refractive index (n) at the ruby frequency ν, the velocity of sound v_s can be calculated by using the expression

$$\Delta\nu = 2\nu v_s n/c \cdot \sin\theta/2 \qquad (9)$$

where $\theta = 180°$. This is also tabulated in Table II. Assuming no dispersion in the velocity of sound, one can also calculate the Brillouin shift at the Nd-laser wavelength of 1.06 μ by using the appropriate refractive index in (9). These values are given in the last column of Table II.

No correlation was found between these shifts and the spacing of lines occurring in the spectra of self-Q-switched outputs. On this basis one can therefore rule out stimulated Brillouin scattering as the mechanism responsible for self-Q-switching. A more likely explanation of the phenomenon resides in the formation of refractive index gratings recently discussed by Key *et al.* [27].

C. Stimulated Raman Scattering: Self-Generated

The internal generation of Raman scattering in a liquid laser has been briefly reported by Alfano and Shapiro [7] and by Land *et al.* [28].

The experimental set up in the present work is shown on Fig. 10. It consisted of a 25-cm cell of 1 cm^2 cross section placed in a dual elliptical cavity. Up to 2500 J could be discharged through two flashlamps. The cavity was formed by a 10-m radius, fully reflecting mirror, and a 50 percent reflecting flat mirror separated by 70 cm. The external surfaces of cell windows were cut at the Brewster angle, and the output mirror was wedged to reduce subsidiary resonances in the cavity. Since the refractive indices of quartz (1.45) and Nd^{3+}:$POCl_3$ (1.452) match quite well, no reflection is obtained from the quartz-solution interfaces; as a consequence, the inner surfaces of the windows can be parallel to each other, greatly simplifying the cell construction.

The laser could be operated in three different regimes: Q switched by a saturable absorber (Kodak 9860 dye); mode locked by suitably adjusting the concentration of the same dye; and self-Q-switched by removing the dye

TABLE II
BRILLOUIN SHIFTS, REFRACTIVE INDICES, AND VELOCITY OF SOUND IN LASER SOLUTIONS

Material	$\Delta\nu$(6942) (cm^{-1})	n 6942 Å	n 10660 Å	V_s (cm/s)	$\Delta\nu$(10600) (cm^{-1})
$SeOCl_2$	0.178	1.6396	1.6249	1130	0.115
$POCl_3$	0.117	1.4559	1.4501	837	0.076
$SnCl_4$	0.116	1.5042	1.4952	803	0.075
$SeOCl_2$:$SnCl_4$	0.178	1.6416	1.6268	1129	0.114
$POCl_3$:$SnCl_4$	0.147	1.457[a]	1.452[a]	1050	0.096
$SeOCl_2$:$SnCl_4$:Nd^{+3}[b]	0.19	1.6650	1.6499	1188	0.123
$POCl_3$:$SnCl_4$:Nd^{+3}	0.18	1.480[a]	1.475[a]	1266	0.117

[a] Estimated values based on increase of refractive index of $SeOCl_2$ upon addition of $SnCl_4$ and Nd.
[b] 0.3 molar concentration of neodymium.

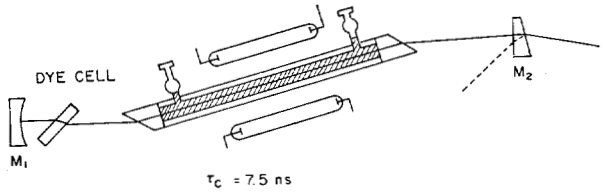

Fig. 10. Schematic arrangement of a mode-locked liquid laser.

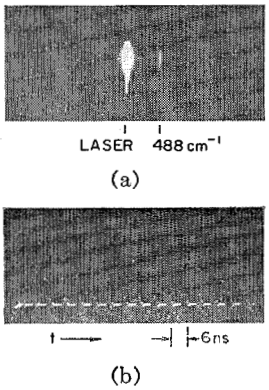

Fig. 11. (a) Mode-locked Nd:$POCl_3$ laser output showing stimulated Raman line. (b) Time output on a Tektronix 519 oscilloscope.

cell and replacing the ouput reflector by an uncoated quartz wedge. The output of the laser was directed into either a 2-m Bausch and Lomb or a ¾-m Jarrell–Ash spectrograph and recorded on sensitized Kodak 12 plates or Polaroid 57 film. A planar photodiode and Tektronix 519 oscilloscope was used to monitor the time dependence of the output.

The Nd^{3+}:$POCl_3$ laser showed stimulated Raman scattering in all three modes of operation. Figs. 11 and 12 show a spectrum and an oscilloscope trace obtained with a mode-locked laser that had a pulse duration of 3 ps and produced Raman scattering with every shot. The stimulated first Stokes line at 488 cm^{-1} is clearly visible. In other spectrograms the second Stokes line was also sometimes detected. The lasting band of about 100 cm^{-1} width is devoid of any structure except for a sharp line of about 2 cm^{-1} width, positioned to the left of the center of the band. The SRS lines were also structureless and of about the same 100 cm^{-1} width. The position of the center of the Raman emission shifts within 10 cm^{-1} from shot to shot with respect to the center of the lasing band. Since not all the pulses in the mode-locked train produce Raman scattering there should not necessarily be exact agreement between the laser bandwidth, which contains the spectrum of all the pulses, and the SRS bandwidth, which contains the spectrum of only some of them. The Raman conversion to first Stokes was measured by placing neutral density filters over the film at the location of the laser line and attenuating it until it reached the same intensity as the Raman line. By calibrating the film spectral response with a tungsten lamp at conversion of approximately 12 percent (into the first Stokes) was obtained. Spectra and oscilloscope traces obtained in the self-Q-switched mode of operation are shown in Fig. 13. In this case SRS appeared only on the most intense shots but contrary to the mode-locked case contained anti-Stokes lines as well.

With $Nd^{+3}SeOCl_2$ solutions we were able to obtain Raman generation only in the mode-locked regime. An example is given in Fig. 14. When regular trains of pulses were emitted (a rather exceptional case with $SeOCl_2$) the first and sometimes the second Stokes lines (386 cm^{-1}) were detected. The laser and Raman emission both occurred over a narrow band of approximately 6 cm^{-1}. The pulse duration measured by two-photon fluorescence was 6 ps. The narrower bandwidth and longer pulse duration can be attributed to the presence of reflections at the parallel liquid-window interfaces, which is larger than for $POCl_3$ because of poorer refractive index matching ($SeOCl_2$–1.67; quartz–1.45). The presence of parallel reflecting surfaces in the cavity is known to cause bandwidth narrowing and pulse lengthening [7].

V. DISCUSSION

The measurements of spontaneous Raman cross sections reported in Section III can be used to calculate the gain of the stimulated process that in turn can be com-

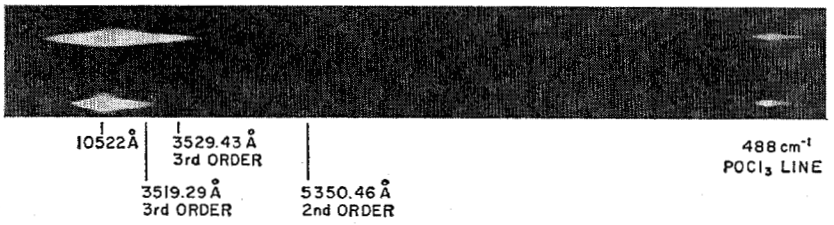

Fig. 12. Spectra of mode-locked Nd:$POCl_3$ liquid laser. Two shots show ≃100 cm^{-1} central band and Raman shifted light.

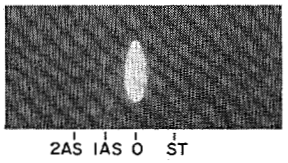

(a)

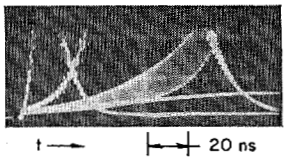

(b)

Fig. 13. (a) Self-Q-switched spectrum showing Stokes and anti-Stokes Raman scattering. (b) Time output on a Tektronix 519 oscilloscope.

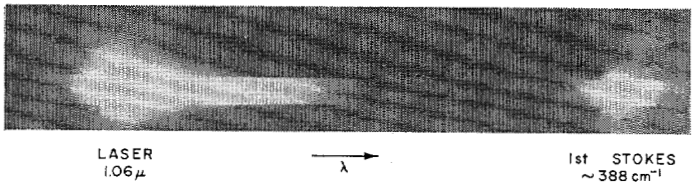

Fig. 14. Stimulated Raman scattering from Nd^{+3}:$SeOCl_2$:$SnCl_4$ laser Q switched with a dye.

pared with the directly measured values of the gain. The gain coefficient g defined by (8) is given by [29]

$$g = \frac{8\pi cN}{\hbar\omega_s^3 n\,\Delta\nu}\left(\frac{d\sigma}{d\Omega}\right)_N \tag{10}$$

where ω_s is the angular frequency of the first Stokes line and the other symbols have their usual meanings.

Using (10) we can calculate the gain coefficient g for $POCl_3$. The measured and calculated values are tabulated in Table I. We see that they agree within ten percent. This close agreement constitutes a strong proof that at the power levels used in SRS (150 MW/cm^2) there is no evidence for self-focusing. This confirms the earlier result (Section III), which showed absence of filaments on photographs, and indicates that the beam quality of liquid lasers is not likely to deteriorate from self-focusing—at least up to these power levels.

A knowledge of the gain for SRS permits us to make an estimate of the limitation imposed by scattering on the performance of liquid amplifiers. The question that we would like to answer is how much of the signal that is fed into an amplifier is likely to be converted into Raman scattering at the output of the device. Since we assume that the stimulated scattering will be generated from noise in the amplifier medium (the input does not contain any Stokes radiation), an accurate calculation is far from trivial and in fact cannot be obtained without approximations in an analytic form. To obtain an estimate, let us refer to Fig. 15, which shows a cell of length l and cross-sectional area A, filled with the liquid laser medium and traversed by a beam from another laser. The amount of Raman flux produced in the element dx and directed so that it will pass through the right window of the cell can be written as

$$dI_R = N\left(\frac{d\sigma}{d\Omega}\right)_N I_L \frac{A}{x^2} e^{gI_L x}\,dx. \tag{11}$$

Since Raman flux generated near the entrance window (left) will experience the greatest gain, we can replace x by l in the solid angle (A/x^2). Upon integration we obtain

$$I_R \approx N\left(\frac{d\sigma}{d\Omega}\right)_N \frac{A}{l^2}\frac{1}{g} e^{gI_L l}. \tag{12}$$

Using quantities characteristic of the experiment that lead to Fig. 6 ($l = 50$ cm, $A - 1$ cm^2, $\lambda = 6940$ Å) and an input $I_L = 100$ MW/cm^2, we obtain $I_R \approx 2 \times 10^{-3}$ MW/cm^2, which is about three orders of magnitude less than what is observed. This result leads us to believe that the relatively high SRS output shown in Fig. 6 is the result of residual feedback that changes the cell from a Raman noise amplifier to a multiple-pass oscillator.[2] This possibility makes it very important to eliminate optical feedback whenever a liquid is used as an amplifier. This is, of course, standard practice even if no SRS is generated. With good design, SRS from liquid amplifiers should not impose any limitations at power inputs in the 100–200 MW/cm^2 range.

Self-generation of SRS in liquid laser oscillators will be governed by similar consideration. Here the problem is somewhat more critical since it imposes a condition

[2] An alternative explanation would be that self-focusing does occur in the cell. This, however, would contradict the remarkable agreement between calculated and measured gains cited above.

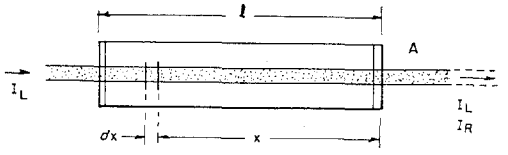

Fig. 15. Geometry leading to (11). Laser beam of intensity I_L traverses a cell of length l and cross sectional area A, and produces a single-pass Raman output I_R.

on the resonator mirrors to have optimum reflectivity for the fundamental and essentially zero reflectivity for the Raman frequencies. The difficulty in observing Raman emission under Q-switched conditions indicates, however, that no serious loss due to SRS does occur at power levels of 100 MW/cm^2.

A somewhat different picture is presented in the case of very high-peak-power picosecond pulses where SRS emission accompanies every shot and conversion efficiencies to SRS of 12 percent have been measured. Quantitative estimates of the conversion would require the use of transient gain equations [30] and a knowledge of dispersion effects. Additional data on thresholds and gains would be needed to warrant such treatment.

In conclusion, we would like to emphasize that results presented in this paper were obtained using stationary (not flowing) liquid laser media. The natural regime of operation of these devices is in the flowing mode, which greatly improves the reproducibility of results. The technology of flowing Nd liquid lasers only recently has been developed, and as their levels of performance climbs to higher values, the effects of nonlinear properties of the medium will become more clearly defined.

Acknowledgment

The authors wish to express their thanks to K. French for providing liquid laser solutions and information on their chemistry, to C. Fallier who took most data on Brillouin scattering, and to T. Illing and S. Hussain who assisted in all phases of the experimental work.

References

[1] A. Lempicki and H. Samelson, "Rare-earth liquid lasers," *Ann. N. Y. Acad. Soc.*, vol. 168, 1970, pp. 596–609.
[2] H. Samelson, R. Kocher, T. Waszak, and S. Kellner, "Oscillator and amplifier characteristics of lasers based on Nd^{+3} dissolved in aprotic solvents," *J. Appl. Phys.*, vol. 41, 1970, pp. 2459–2469.
[3] C. Brecher and K. French, "Comparison of aprotic solvents for Nd^{3+} liquid laser systems: selenium oxychloride and phosphorous oxychloride," *J. Phys. Chem.*, vol. 73, 1969, pp. 1785–1789.
[4] H. Samelson, A. Lempicki, and V. Brophy, "Self-Q-switching of the Nd^{3+} $SeOCl_2$ liquid laser," *J. Appl. Phys.*, vol. 39, 1968, pp. 4029–4030.
[5] G. Yamaguchi, F. Endo, S. Murakawa, S. Okamura, and C. Yamanaka, *Japan. J. Appl. Phys.*, vol. 7, 1968, pp. 179–180.
[6] H. Samelson and A. Lempicki, "Q-switching and mode-locking of Nd^{3+}:$SeOCl_2$ liquid laser," *J. Appl. Phys.*, vol. 38, 1968, pp. 6115–6116.
[7] R. R. Alfano and S. L. Shapiro, "Picosecond pulse emission from a mode-locked Nd^{3+} $POCl_3$ liquid laser," *Opt. Commun.*, vol. 2, 1970, pp. 90–92.
[8] G. Eckhardt, R. Hellwarth, F. J. McClung, S. E. Schwarz, D. Weiner, and E. J. Woodbury, "Stimulated Raman scattering from organic liquids," *Phys. Rev. Lett.*, vol. 9, 1962, pp. 455–457.
[9] A. J. DeMaria, D. A. Stetser, and H. Heynau, "Self-mode-locking of laser with saturable absorbers," *Appl. Phys. Lett.*, vol. 8, 1966, pp. 174–176.
[10] J. P. Laussade and A. Yariv, "Mode-locking and ultra-short laser pulses by anisotropic molecular liquids," *Appl. Phys. Lett.*, vol. 13, 1968, pp. 65–66.
[11] J. Comly, E. Garmire, J. P. Laussade, and A. Yariv, "Observation of mode-locking and ultrashort optical pulses induced by anisotropic molecular liquids," *Appl. Phys. Lett.*, vol. 13, 1968, pp. 176–178.
[12] G. Nagarajan and A. Muller, "Thermodynamische funktionen and molekulare polarisierbarkeiten von thionyl und seleninylhalogeniden," *Z. Naturforsch., A*, vol. 216, 1966, pp. 612–617.
[13] H. Gerding, E. Smit, and R. Westrik, "Die ramanspektren und die molekulstrukturen des selenoxychlorids und des thionylchlorids," *Rec. Trav. Chim.*, vol. 60, 1941, pp. 514–522.
[14] D. Kato, "Raman spectroscopy in the $SeOCl_2$–$SnCl_4$ liquid," *J. Phys. Soc. Jap.*, vol. 29, 1970, p. 1103.
[15] G. Herzberg, *Molecular Spectra and Molecular Structure II Infrared and Raman Spectra of Polyatomic Molecules*. Princeton, N. J.: Van Nostrand, 1968, p. 277.
[16] T. C. Damen, R. C. C. Leite, and S. P. S. Porto, "Angular dependence of the Raman scattering from benzene excited by the He-Ne cw laser," *Phys. Rev. Lett.*, vol. 14, 1965, pp. 9–11.
[17] L. Nafie, P. Stern, B. Fanconi, and W. L. Peticolas, "Angular dependence of Raman scattering intensity," *J. Chem. Phys.*, vol. 52, 1970, pp. 1584–1588.
[18] F. J. McClung and D. Weiner, "Measurement of Raman scattering cross-section for use in calculating stimulated Raman scattering effects," *J. Opt. Soc. Amer.*, vol. 54, 1964, pp. 641–644.
[19] W. R. L. Clements and B. P. Stoicheff, "Raman linewidth for stimulated threshold and gain calculations," *Appl. Phys. Lett.*, vol. 12, 1968, pp. 246–248.
[20] E. M. Garmire, "An investigation of stimulated Raman emission," Ph.D. dissertation, Mass. Inst. Technol., Cambridge, Mass., 1965.
[21] R. H. Pantell and H. E. Puthoff, *Fundamentals of Quantum Electronics*. New York: Wiley, 1969, p. 240.
[22] K. French, private communication.
[23] N. Bloembergen, "The stimulated Raman effect," *Amer. J. Phys.*, vol. 35, 1967, pp. 989–1023.
[24] S. L. Shapiro, J. A. Giordmaine, and K. W. Wecht, "Stimulated Raman and Brillouin scattering with picosecond light pulses," *Phys. Rev. Lett.*, vol. 19, 1967, pp. 1093–1095.
[25] R. R. Alfano and S. L. Shapiro, "Emission in the region 4000 to 7000 Å via four-photon coupling in glass," *Phys. Rev. Lett.*, vol. 24, 1970, pp. 584–585.
[26] R. G. Brewer and D. C. Shapero, "Multiple stimulated Brillouin scattering," in *1965 Proc. Phys. Quantum Electron. Conf.*, San Juan, Puerto Rico, P. L. Kelly, B. Lax, and P. E. Tannenwald, Eds. New York: McGraw-Hill, 1966, pp. 216–221.
[27] P. Y. Key, R. G. Harrison, V. I. Little, and J. Katzenstein, "Bragg reflection from a phase grating induced by nonlinear optical effects in liquids," *IEEE J. Quantum Electron.*, vol. QE-6, Oct. 1970, pp. 641–646.
[28] R. S. Lang, H. Baumhacker, and E. E. Fill, "Stimulated Raman scattering in an inorganic Nd liquid laser," *Phys. Lett.*, vol. 32A, 1970, pp. 433–434.
[29] M. Maier, W. Kaiser, and J. A. Giordmaine, "Backward stimulated Raman scattering," *Phys. Rev.*, vol. 177, 1969, pp. 580–599.
[30] R. L. Carman, M. E. Mack, F. Shimizu, and N. Bloembergen, "Forward picosecond Stokes-pulse generation in transient stimulated Raman scattering," *Phys. Rev., Lett.*, vol. 23, 1969, pp. 1327–1329.